

# Cellulose-Based Fully Green Triboelectric Nanogenerators with Output Power Density of $300 \text{ W m}^{-2}$

Renyun Zhang,\* Christina Dahlström,\* Haiyang Zou, Julia Jonzon, Magnus Hummelgård, Jonas Örtégren, Nicklas Blomquist, Ya Yang, Henrik Andersson, Martin Olsen, Magnus Norgren, Håkan Olin, and Zhong Lin Wang\*

**Triboelectric nanogenerators (TEGs) have attracted increasing attention because of their excellent energy conversion efficiency, the diverse choice of materials, and their broad applications in energy harvesting devices and self-powered sensors. New materials have been explored, including green materials, but their performances have not yet reached the level of that for fluoropolymers. Here, a high-performance, fully green TENG (FG-TENG) using cellulose-based tribolayers is reported. It is shown that the FG-TENG has an output power density of above  $300 \text{ W m}^{-2}$ , which is a new record for green-material-based TENGs. The high performance of the FG-TENG is due to the high positive charge density of the regenerated cellulose. The FG-TENG is stable after more than 30 000 cycles of operations in humidity of 30%–84%. This work demonstrates that high-performance TENGs can be made using natural green materials for a broad range of applications.**

Such demand brings about environmental anxieties, and thus, environmentally friendly materials<sup>[12]</sup> are preferred for future development of TENGs. Efforts have been made to utilize biodegradable materials such as nanocellulose<sup>[13–15]</sup> and dissolved cellulose.<sup>[16]</sup>

Cellulose is generally considered to have a low triboelectric effect<sup>[15]</sup> because of its low charge affinity. Therefore, a few studies<sup>[14,15,17,18]</sup> have been carried out using cellulose materials as tribolayers. However, a recent study<sup>[19]</sup> has indicated that cellulose acetate has a higher triboelectric effect than polytetrafluoroethylene (PTFE). This finding implies the great potential of cellulose-based materials<sup>[20]</sup> for use in environmentally friendly TENGs<sup>[21]</sup>

with performances close to those using fluoropolymers.

Reports on green TENGs using environmentally friendly materials have been presented.<sup>[12,22]</sup> However, a green TENG should consider not only the tribolayers<sup>[13–16,23]</sup> but also the back electrodes. The back electrodes are commonly metals such as gold,<sup>[24,25]</sup> copper,<sup>[26–29]</sup> or aluminum.<sup>[30–32]</sup> These metal electrodes are usually sputtered on the tribolayers, which limits their applications in large-scale production. Alternatives to metals include carbon materials, such as graphene,<sup>[22,23,33]</sup> that are more environmentally friendly.

Triboelectric nanogenerators (TEGs) have demonstrated promising applications in energy harvesting from different recourses such as mechanical vibrations,<sup>[1]</sup> water-droplet,<sup>[2]</sup> wind,<sup>[3]</sup> sound,<sup>[4]</sup> and even ultrasound.<sup>[5]</sup> The basic mechanism behind TENGs is the triboelectrification<sup>[6]</sup> of two tribolayers with different charge polarities.<sup>[7]</sup> Such an essential mechanism implies that the energy output of TENGs is based on the triboelectric effects<sup>[8]</sup> and the structure of the contact area<sup>[9]</sup> of the tribolayers. Therefore, large-area triboelectric materials are in high demand to produce massive energy using TENGs.<sup>[10,11]</sup>

Dr. R. Y. Zhang, J. Jonzon, Dr. M. Hummelgård, Dr. J. Örtégren,  
Dr. N. Blomquist, Dr. M. Olsen, Prof. H. Olin  
Department of Natural Sciences  
Mid Sweden University  
Holmgatan 10, Sundsvall SE-85170, Sweden  
E-mail: renyun.zhang@miun.se

Dr. C. Dahlström, Prof. M. Norgren  
FSCN  
Surface and Colloid Engineering  
Mid Sweden University  
Holmgatan 10, Sundsvall SE-85170, Sweden  
E-mail: christina.dahlstrom@miun.se

Dr. H. Y. Zou, Prof. Z. L. Wang  
School of Materials Science and Engineering  
Georgia Institute of Technology  
Atlanta, GA 30332-0245, USA  
E-mail: zlwang@gatech.edu

Prof. Y. Yang, Prof. Z. L. Wang  
Beijing Institute of Nanoenergy and Nanosystems  
Chinese Academy of Sciences  
Beijing 100083, P. R. China

Dr. H. Andersson  
Department of Electronics Design  
Mid Sweden University  
Holmgatan 10, Sundsvall SE-85170, Sweden

 The ORCID identification number(s) for the author(s) of this article can be found under <https://doi.org/10.1002/adma.202002824>.

© 2020 The Authors. Published by Wiley-VCH GmbH. This is an open access article under the terms of the Creative Commons Attribution License, which permits use, distribution and reproduction in any medium, provided the original work is properly cited.

DOI: 10.1002/adma.202002824

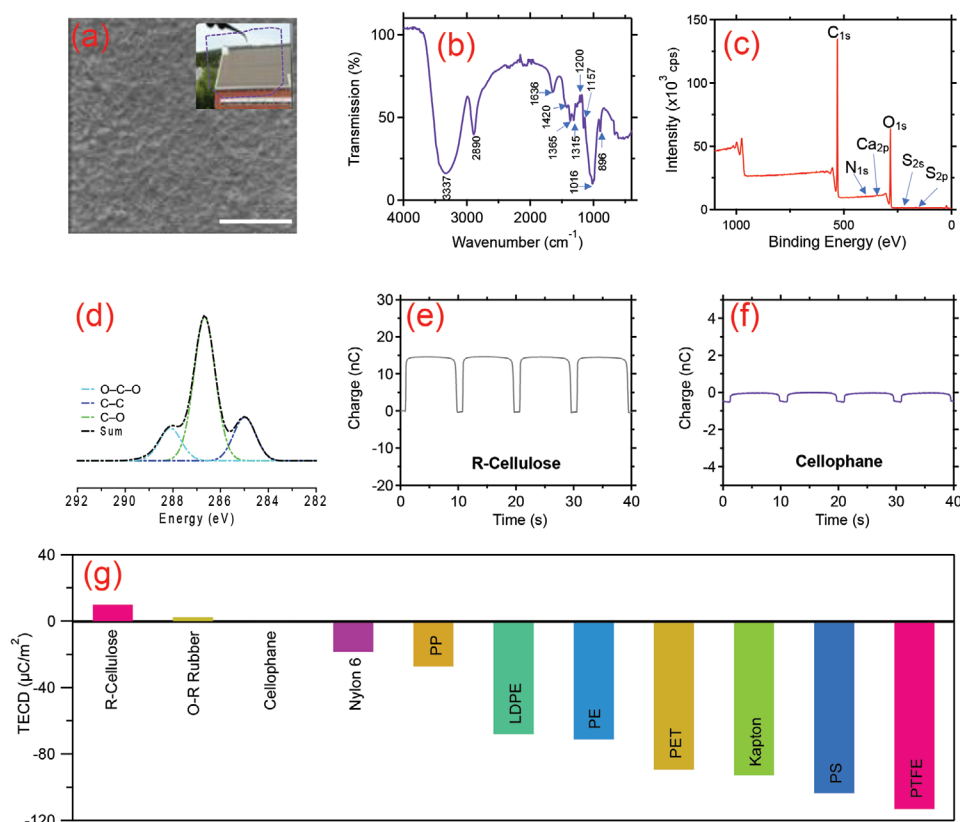


**Figure 1.** Characterization of R-cellulose and cellophane films. a) An SEM image and a photograph of a 20  $\mu\text{m}$  R-cellulose film showing the surface morphology and transparency; scale bar in the SEM image: 2  $\mu\text{m}$ . b) FTIR spectra of the R-cellulose film. c) XPS spectra of the R-cellulose film. d)  $\text{C}_{1s}$  XPS spectra of R-cellulose showing the bands of O—C—O, C—C, and C—O typical for cellulose. e) Measured signal in the TECD experiment on R-cellulose. f) Measured signal in the TECD experiment on cellophane. g) Quantified triboelectric series, showing R-cellulose, cellophane, oil-resistant Buna-N rubber, nylon 6, polypropylene (PP), low-density polyethylene (LDPE), polyethylene (PE), polyester (PET), Kapton, polystyrene (PS), and poly(tetrafluoroethylene) (PTFE).

Here, we report a fully green TENG (FG-TENG) using cellulose-based material such as regenerated cellulose (R-cellulose) and commercial cellophane as tribolayers and graphite foils as electrodes. The power density of the FG-TENG is  $307 \text{ W m}^{-2}$ , which is in the same order of fluoropolymer-based TENGs.<sup>[34,35]</sup> With such a high power density, a  $40 \text{ cm}^2$  FG-TENG can be used for continuously powering an emergency indicator and commercial decoration light-emitting diode (LED) lamps. This work demonstrates that a high-output TENG can be made with only green materials, which will be a new strategy for future research and development.

The R-cellulose was produced in our laboratory using an environmentally friendly method.<sup>[36–38]</sup> A  $20 \mu\text{m}$  thick flexible and transparent film (Figure 1a) with a density of  $1.4 \text{ g cm}^{-3}$  was made from dissolved cellulose. The surface of the film was characterized by scanning electron microscopy (SEM) in secondary electron (SE) mode (Figure 1a). Cross-sectional image of the R-cellulose film is given in Figure S1 (Supporting Information). The Fourier transform infrared spectroscopy (FTIR) spectra of the film is given in Figure 1b, showing bands at  $896 \text{ (C—O—C)}$ ,  $1016 \text{ (C—OH)}$ ,  $1157 \text{ (C—C)}$ ,  $1200 \text{ (C—OH, C—CH)}$ ,  $1315 \text{ (C—H)}$ ,  $1365 \text{ (C—H)}$ ,  $1420 \text{ (C—H)}$ ,  $1636 \text{ (adsorbed water)}$ ,  $2890 \text{ (C—H)}$  and  $3337 \text{ (O—H)} \text{ cm}^{-1}$  that correspond to the chemical structure of cellulose.

The mechanical properties of the R-cellulose were also measured, and the results indicate that the  $20 \mu\text{m}$  thick film

is very strong with an elastic modulus of  $78 \text{ GPa}$ , a stiffness of  $73.4 \text{ N mm}^{-1}$  and a specific stress (Figure S2, Supporting Information) of  $80.2 \text{ kN m kg}^{-1}$ . Such mechanical strength of the film is among the highest for polymers.<sup>[39]</sup> With such great mechanical stability, the R-cellulose film can withstand mechanical friction when used as a tribolayer in TENGs.

The X-ray photoelectron spectroscopy (XPS) spectra of the R-cellulose film are given in Figure 1c. Residual-XPS-peaks of  $\text{N}_{1s}$ ,  $\text{Ca}_{2p}$ ,  $\text{S}_{2s}$ , and  $\text{S}_{2p}$  were detected in the film, which were from the material processing procedures. Figure 1d shows the  $\text{C}_{1s}$  XPS spectra of the R-cellulose, showing O—C—O, C—C, and C—O bands of cellulose.

The triboelectric charge densities (TECDs) of the R-cellulose and cellophane were measured using a recently reported method.<sup>[19]</sup> The TECD for R-cellulose is  $+10.05 \mu\text{C m}^{-2}$  (Figure 1e), which is very positive and three times that of oil-resistant Buna-N rubber ( $2.95 \mu\text{C m}^{-2}$ ). The TECD for cellophane is  $0.17 \mu\text{C m}^{-2}$  (Figure 1f). Figure 1g shows the triboelectric order of R-cellulose, cellophane and other commonly used triboelectric materials. The results indicate that the TECD of R-cellulose is almost 60 times that of cellophane, suggesting a high triboelectrification between these two materials and thus a good pair of materials for fabricating a TENG.

To fabricate an FG-TENG, both R-cellulose and cellophane were adhered onto graphite foils. Figure 2a shows a schematic

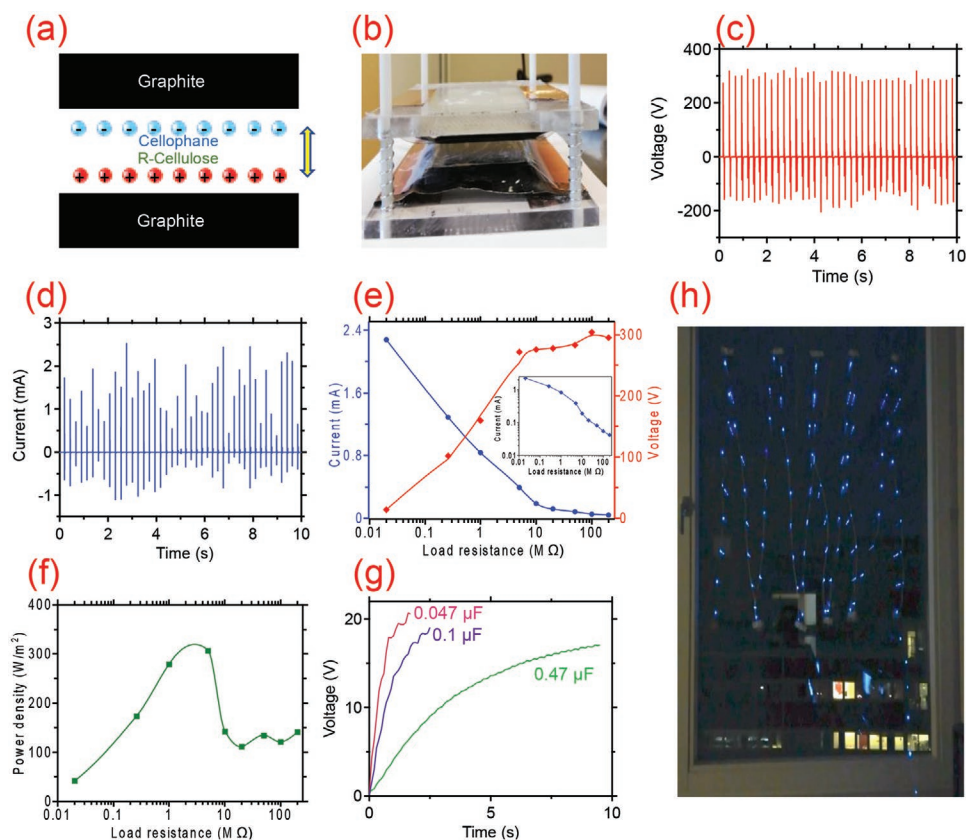


**Figure 2.** FG-TENG. a) Schematic drawing of the construction of the FG-TENG. b) Photograph of the fabricated FG-TENG. c) Open-circuit voltage measured on the FG-TENG. d) Short-circuit current measured on the FG-TENG. e) Current and voltage measured at different load resistances from 20 k $\Omega$  to 200 M $\Omega$ . The insert shows the current with a logarithmic axis. f) Output power density of the FG-TENG at different loads. g) Potential changes of different capacitors charged by the FG-TENG. h) Photograph of a window decoration lamp curtain lighted by the FG-TENG. The FG-TENG was operated manually by hands for the results presented in this figure.

drawing of the structure of the TENG, and a photograph is shown in Figure 2b. As mentioned above, R-cellulose has a higher positive charge density than cellophane. Therefore, electrons transfer from the R-cellulose to the cellophane.

Electrical measurements show that the FG-TENG operated manually in the contact-separation mode has an open-circuit voltage of up to 300 V and a short-circuit current of up to 2.6 mA (Figure 2c,d). The results of the voltage and current changes with different loads connected to the FG-TENG circuit are given in Figure 2e. The output power density of the FG-TENG (5  $\times$  5 cm<sup>2</sup>) is shown in Figure 2f, indicating a density of 307 W m<sup>-2</sup> at a load resistance of 5 M $\Omega$ . The high output of the FG-TENG can be used to light commercial decoration lamps with 100 LEDs (Figure 2h). The experiment here was done manually by hands.

Another experiment (Figure S3, Supporting Information) of a 3  $\times$  3 cm<sup>2</sup> FG-TENG was performed on a linear motor, giving a power density of 98 W m<sup>-2</sup> at a contact speed of 1 m s<sup>-1</sup>. The current and power density at different contact speeds are given in Figure S4 (Supporting Information).

To quantitatively measure the energy output, we connected a capacitor (0.47  $\mu$ F) to the FG-TENG circuit to measure the actual charges stored at different contact-separation frequencies. The results indicate that the FG-TENG can generate

68  $\mu$ J in 10 s at a frequency of 5 Hz. Moreover, we used the FG-TENG to charge three capacitors with different capacitances (Figure 2g). At a contact-separation frequency of 7 Hz, a 0.047  $\mu$ F capacitor can be charged to 21 V in 2 s, while this value is 19 V in 2.5 s for a 0.1  $\mu$ F capacitor and 17 V in 10 s for a 0.47  $\mu$ F capacitor. Figure S5 (Supporting Information) shows the results of charging a 0.47  $\mu$ F capacitor at different frequencies.

In order to study the output of the FG-TENG at high load resistance, we charged a 0.47  $\mu$ F capacitor using the FG-TENG where a 1 G $\Omega$  resistor is serially connected (Figure S6, Supporting Information). Results show that the capacitor can be charged to 0.8 V after 70 contact-separation cycles, giving a total stored energy of 0.16  $\mu$ J. We have also serially connected 28 LEDs to the resistor and then to the FG-TENG through a rectifier. The results (Figure S6 and Video S1, Supporting Information) show that the LEDs can be easily lighted by the FG-TENG, indicating the high performance of the FG-TENG.

We have also studied the FG-TENG performed on a sliding mode. Results (Figure S7, Supporting Information) show that the maximum open circuit voltage was around 350 V, and the short circuit current was 967  $\mu$ A. Power output of the sliding mode has a maximum value of 2.1 mW at a load of 1 M $\Omega$ .

In addition to the high performance, the stability of the FG-TENG was also studied in our experiments. The stability

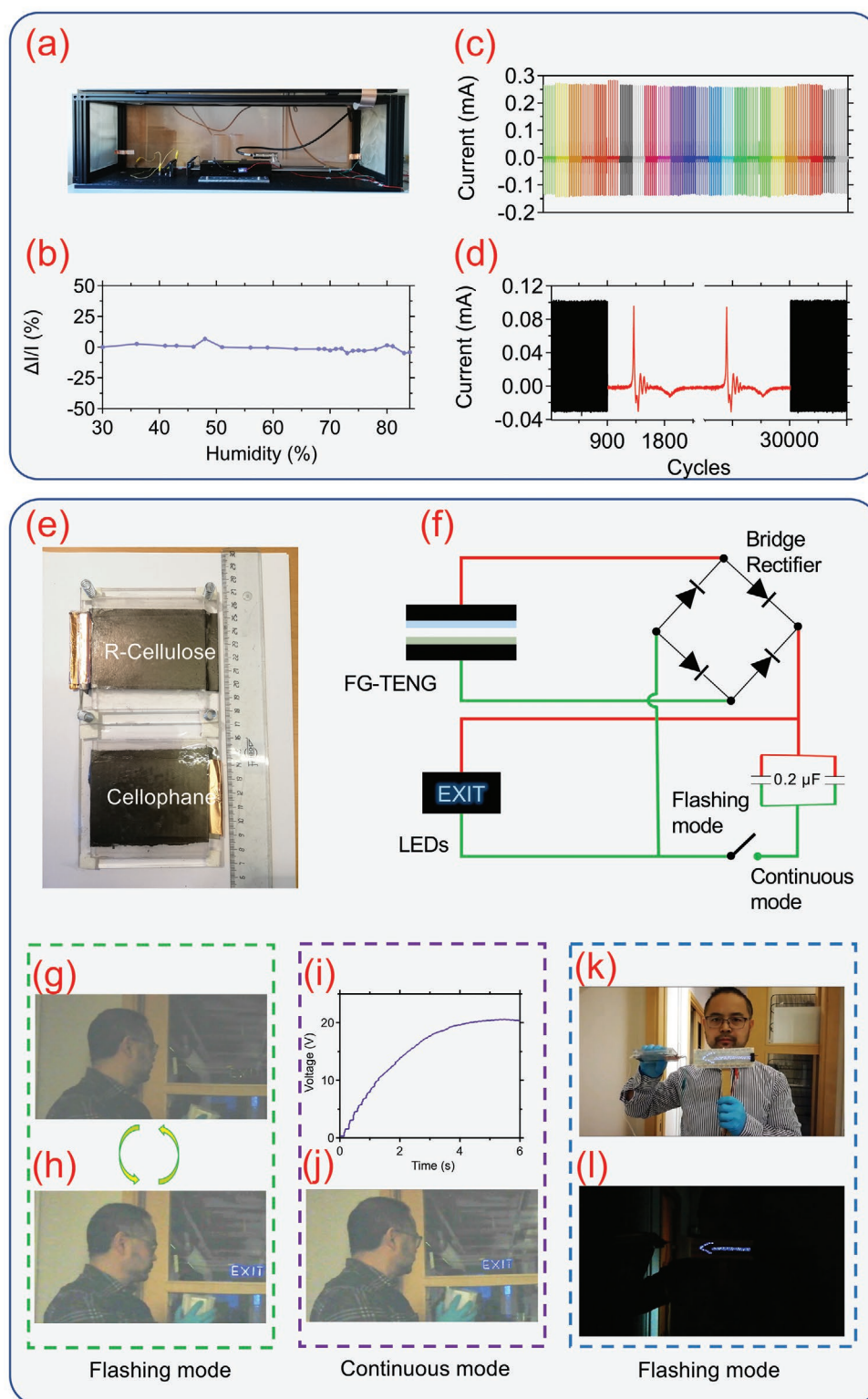


**Figure 3.** Stability and applications of the FG-TENG. a) Photograph of the test system including the chamber, linear motor, and FG-TENG. b) Change in the short-circuit signal at humidity of 30%–84%. c) Measured short-circuit current, corresponding to the points in (b). d) Short-circuit current of the FG-TENG under 30 900 operational cycles at a frequency of 18 Hz. The insert shows the shape of the signals. The FG-TENG was operated by a linear motor for the results presented in (b–d). e) Photograph of the components of the FG-TENG. f) Circuit for lighting an emergency “EXIT” indicator using the FG-TENG. g, h) Two photographs showing the “EXIT” sign lit up under flashing mode. i) Voltage measured on the capacitors when charging with the FG-TENG. j) Photograph showing the “EXIT” sign lit up under continuous mode. k) Photograph of an arrow shape indicator powered by the FG-TENG at full illumination. l) Photograph of the arrow shape indicator powered by the FG-TENG in the dark.

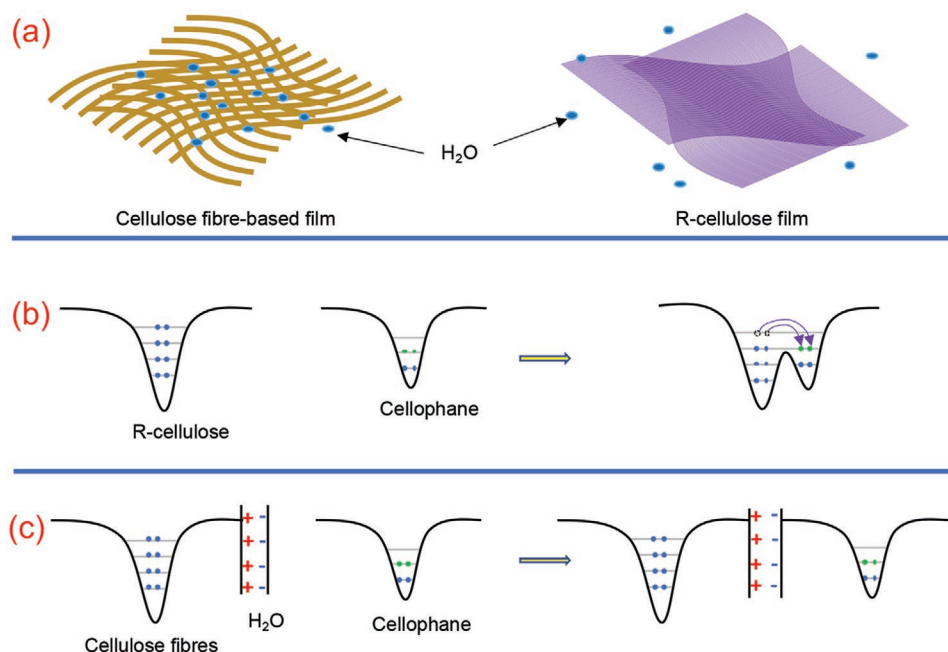


**Figure 4.** a) Schematic drawing showing the difference of water diffusion in the cellulose fiber-based film and the R-cellulose film. b,c) Electron-potential-well model of the triboelectrification of R-cellulose film and cellulose fiber-based film. b) the triboelectrification of R-cellulose before and in contact with cellophane. c) The triboelectrification of cellulose fiber-based film before and in contact with cellophane.

of the FG-TENG was tested with a linear motor mounted in a chamber (Figure 3a). First, we tested the stability of the FG-TENG at different humidity, and the results indicate that it is not sensitive to humidity from 30% to 84% as tested. The signal change of the short-circuit current is less than 5% (Figure 3b,c). The reason for this phenomenon is the high density of the R-cellulose film, which will be discussed below. Second, we tested the stability of the output (Figure 3d), and the results clearly show that no obvious output decrease occurs after 30 900 cycles.

To demonstrate the application of the FG-TENG in practice, the circuit of the device was redesigned (Figure 3e,f) to power an emergency “EXIT” indicator. Two parallel connected capacitors (0.1  $\mu\text{F}$ ) were connected to the circuit, and a switch was added after the capacitors. This design allows the system to show different signals in either a flashing mode or a continuous mode. If the switch is open, then “EXIT” will flash (Figure 3g,h) because of the pulse current from the FG-TENG. If the switch is closed, then the output from the FG-TENG will first charge the capacitors (Figure 3i) and then light the “EXIT” sign (Figure 3j). With this circuit, the “EXIT” sign can be lit up at a contact-separation frequency of 1 Hz. Videos of the two modes are given in Videos S2 and S3 (Supporting Information). In another scenario, an arrow indicator being held by a person was lit up (Figure 3k,l) by the FG-TENG. Such indicators can be used in cases where normal illumination is absent. Videos of the two modes are given in Videos S4 and S5 (Supporting Information).

Our findings here have shown that R-cellulose has a high triboelectric effect, which challenges the common belief that cellulose materials are not good triboelectric materials. Commonly used microfibrillated cellulose (MFC) or cellulose nanofibrils (CNF) films are porous materials because they are based on fibers, which means that space exists between

the fibers that allows water molecules to enter and bind to the fibers. Typically the density of CNF films is in the range of 1.2–1.3  $\text{g cm}^{-3}$ .<sup>[40,41]</sup> Moreover, to obtain CNF, a charging up of the cellulose raw material by introduction of carboxylate groups onto the cellulose internal fibrillar surfaces to be able to disperse the nanofibers and to avoid aggregation is necessary.<sup>[42]</sup> Thereby the CNF films will adsorb moisture/water more strongly than underivatized cellulose.<sup>[36,43,44]</sup> The binding of water significantly reduces the triboelectric effect,<sup>[45]</sup> which suggests why the measured triboelectric effects of fibrillated cellulose and paper in most studies are relatively weak. In our experiment, cellulose films were formed from dissolved cellulose polymers that are molecules, not fibers, resulting in films with densities of 1.4  $\text{g cm}^{-3}$ , which is close to the nominal value of pure cellulose: 1.5  $\text{g cm}^{-3}$ . Such a high density indicates that the R-cellulose films are not porous. Dense films inhibit the diffusion and binding of water to the cellulose polymers in the films (Figure 4a), leading to a high triboelectric effect. Figure 4b,c shows a schematic illustration of an electron potential well model of the difference between our R-cellulose and cellulose fibers. The states of bonding electrons in R-cellulose and cellulose fibers are similar since the chemical structures are the same (Figure 4b,c). When R-cellulose gets in contact with cellophane, the energy barrier decreases and lets electrons transfer from R-cellulose to cellophane (Figure 4b). For the case of cellulose fibers/fibrils, the adsorbed water molecules act as barrier (Figure 4c) and block the transfer of electrons. Therefore, the triboelectric effects of porous cellulose fiber or fibril-based films are weaker than R-cellulose and cellulose acetate films that can be made denser.<sup>[19]</sup>

To verify the suggested mechanism, we have measured the output current of a TENG using CNF as a tribolayer. Figure S8

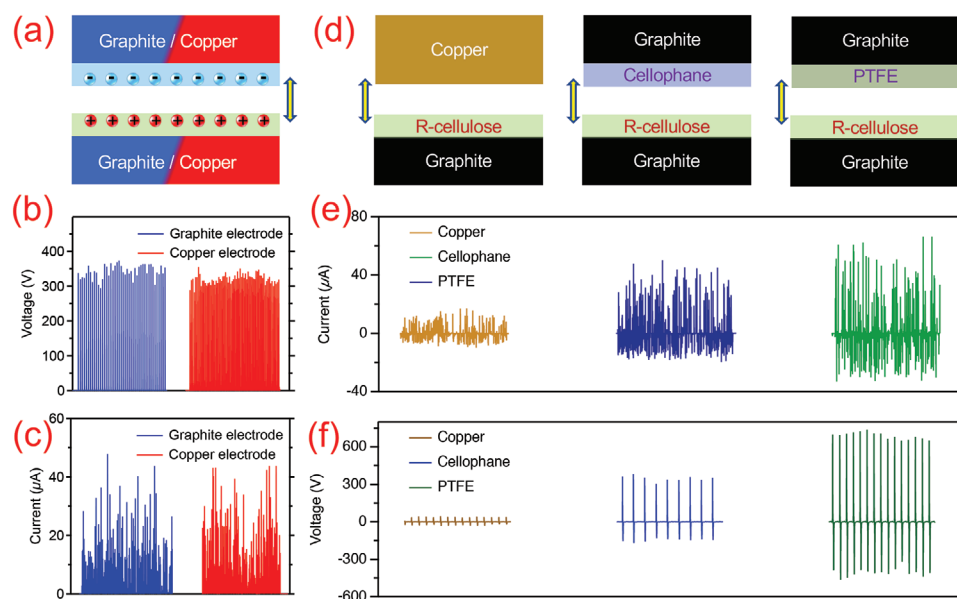


**Figure 5.** Evaluation of the FG-TENG. a) Schematic drawing of an evaluation that compares the graphite electrodes as used in the FG-TENG and copper electrodes. b) Voltage measured on the two TENGs using graphite or copper electrodes. c) Current measured on the two TENGs using graphite or copper electrodes. d) Schematic drawing of an evaluation in which copper, cellophane, and PTFE were used as tribolayers to generate electricity with R-cellulose. e) Current measured on the TENGs using different tribolayers. f) Voltage measured on the TENGs using different tribolayers. The FG-TENG was operated manually for the results presented in this figure. The current signal was measured on a PXI-4132 source measurement unit.

(Supporting Information) shows that the current decreased over 32% when humidity increased from 48% to 62%. The results suggest that moisture can easily diffuse and adsorb to the CNF and creates a barrier on the CNF to block the transfer of electrons. Such a result supported our suggested mechanism above.

It has been observed that piezoelectric effects from cellulosic materials can be attributed if the crystalline regions are properly oriented (anisotropic structures) by application of different external, directional force fields, e.g., direct current electrical fields and/or mechanical alignment by shear etc., when consolidating the films.<sup>[46–48]</sup> Actually, this could also contribute to the generation of high output currents. However, in the present case no such force field have been applied when preparing the R-cellulose, which for that reason is considered isotropically oriented with low strainability. Therefore, the electrical signals measured in our experiment are due to the triboelectric effect of the R-cellulose.

To further evaluate the performance of the FG-TENG, we compared the performance of the FG-TENG with those of other TENGs, using either metal electrodes or noncellulose tribolayers (Figure 5). We first evaluated the impact of the electrode by comparing the graphite electrode and copper electrode (Figure 5a). The results demonstrate that both the open-circuit voltage (Figure 5b) and short-circuit current (Figure 5c) of the FG-TENG are higher than those of the TENG that uses copper electrodes. The maximum output power of the FG-TENG is 35% higher than that of the TENG using copper electrodes. This finding clearly shows that graphite foil has great potential for replacing metal electrodes in TENGs.

We also compared the FG-TENG with two other TENGs, using copper and PTFE as tribolayers instead of cellophane (Figure 5d). The maximum current (Figure 5e) measured in the tests for the three TENGs are 17, 50.1, and 66.5  $\mu\text{A}$ , and the maximum voltages are 47, 383, and 736 V, (Figure 5f). A simple

estimation of the maximum output power using  $P = UI$  indicates that the output of the FG-TENG using cellophane as a tribolayer is 24 times that of the TENG using a copper tribolayer, and  $\approx 40\%$  that of the TENG using PTFE as a tribolayer. These results also indicate that the FG-TENG has an output on the same order of magnitude as was obtained with fluoropolymers.

The maximum output power density of the FG-TENG is  $307 \text{ W m}^{-2}$ , which is in the same order as of fluoropolymer based TENGs.<sup>[34,35]</sup> Such findings will have great impact on the selection of materials in future TENG studies. With further doping or functionalization of the R-cellulose polymers, even higher performance could be achieved. The reason for the expected higher output based on doped or functionalized cellulose materials is that cellulose polymers can be easily modified with either electron donating and accepting functional groups.<sup>[15]</sup> Such modifications allow us to produce cellulose films with either high positive or high negative charge affinities. Our study shows evidence that this concept would work because the cellophane used in our experiment is also a kind of regenerated cellulose material. The results indicate that the output of the FG-TENG is high despite the TECD difference between the R-cellulose and cellophane not being very significant. Therefore, a high possibility exists to make another type of FG-TENG using cellulose-based films with larger TECD differences. Another report by Wang's group has indicated that cellulose acetate has a high negative charge affinity that is even stronger than PTFE.<sup>[19]</sup> These results demonstrate the great potential of cellulose materials in TENG and will have great impact on future studies.

In summary, we have developed a high-output FG-TENG using only cellulose-based materials as tribolayers and graphite foils as electrodes. Such an FG-TENG has shown excellent performance when operated in the contact-separation mode, and the output from the FG-TENG in the same order of

fluoropolymer based TENGs. The study presented here provides a new concept for TENG construction using only green materials. This concept could lead to the development of a new generation of high-performance green TENGs for energy harvesting and self-powered sensing.

## Experimental Section

**Materials:** The cellulose used for dissolution/regeneration was a commercial dissolving pulp from Domsjö Fabriker Aditya Birla (Örnsköldsvik, Sweden). The average molecular weight ( $M_w$ ) was  $3.2 \times 10^5 \text{ g mol}^{-1}$ , and the polydispersity index was 10.3.

Urea ( $\geq 99.5\%$ ) was purchased from Sigma-Aldrich, LiOH-H<sub>2</sub>O (56.5%) from Alfa Aesar and ethanol ( $\geq 99.8\%$ ) from VWR Chemicals.

The cellulose was dissolved according to the reported method.<sup>[36,37]</sup> R-cellulose films were prepared by casting the solution onto glass plates (with a thickness corresponding to the desired thickness in the dry state) and immersed into an ethanol regeneration bath for 2 h. The films were placed in a Milli-Q water bath to wash away the LiOH and urea, and the water was changed daily until pH 7 was reached. The films were dried at room temperature for  $\approx 8$  h; to avoid shrinkage, each film was placed on a plastic plate, and all film edges were taped. The taped edges were cut away after drying.

The cellophane film was purchased from Materialbutiken (Sweden). The graphite foil (F02012TH) was purchased from SGL Group (Germany).

**Characterization:** SEM imaging of the R-cellulose film was performed on a TESCAN MAIA3 electron microscope in SE mode. The FTIR spectrum of the film was obtained on a Nicolet 6700 spectrometer (Thermo Scientific). Mechanical testing of the film was performed on an MTS/4MC using a preload of 0.1 N. The test span used was 3 cm, and the sample width was 1 cm. TECD measurement was performed according to a previously reported method.<sup>[19]</sup>

**Assembly of the FG-TENG:** To assemble the FG-TENG, the R-cellulose and cellophane films were glued (ethyl cyanoacrylate) on graphite foils. The TENG shown in Figure 5a using copper electrodes was assembled by attaching R-cellulose and cellophane films onto two pieces of copper tape. The TENG shown in Figure 5d using PTFE as a tribolayer was simply assembled by attaching the PTFE film onto graphite foil using a cyanoacrylate glue.

**Electrical Measurements:** Electrical signals were measured with a PXI-4071 digital multimeter. The current signals in Figure 5 were measured with a PXI-4132 source measurement unit.

## Supporting Information

Supporting Information is available from the Wiley Online Library or from the author.

## Acknowledgements

This work was financially supported by the European Regional Development Fund, the Energy Agency of Sweden, Stiftelsen Promobilia, Region Västernorrland, Sundsvalls Kommun, Timrå Kommun, and Härnösands Kommun. M.N. thanks the Swedish Research Council (Vetenskapsrådet) and FORMAS for support through research grant nos. 2015-04290 and 942-2015-251, respectively. The author R.Y.Z. consents to his image being published in Figure 3 of this article, as well as its reuse of the image in any future review articles.

## Conflict of Interest

The authors declare no conflict of interest.

## Keywords

green materials, regenerated cellulose, triboelectric charge densities, triboelectric nanogenerators

Received: April 26, 2020

Revised: June 8, 2020

Published online:

- [1] S. Wang, S. Niu, J. Yang, L. Lin, Z. L. Wang, *ACS Nano* **2014**, *8*, 12004.
- [2] J. H. Lee, S. Kim, T. Y. Kim, U. Khan, S.-W. Kim, *Nano Energy* **2019**, *58*, 579.
- [3] J. Bae, J. Lee, S. Kim, J. Ha, B.-S. Lee, Y. Park, C. Choong, J.-B. Kim, Z. L. Wang, H.-Y. Kim, J.-J. Park, U.-I. Chung, *Nat. Commun.* **2014**, *5*, 4929.
- [4] X. Fan, J. Chen, J. Yang, P. Bai, Z. Li, Z. L. Wang, *ACS Nano* **2015**, *9*, 4236.
- [5] R. Hinchet, H.-J. Yoon, H. Ryu, M.-K. Kim, E.-K. Choi, D.-S. Kim, S.-W. Kim, *Science* **2019**, *365*, 491.
- [6] Z. L. Wang, A. C. Wang, *Mater. Today* **2019**, 2019.
- [7] Z. L. Wang, L. Lin, J. Chen, S. Niu, Y. Zi, in *Triboelectric Nanogenerators*, Springer International Publishing, Cham, Switzerland **2016**, pp. 1–19.
- [8] Z. L. Wang, *Nano Energy* **2020**, *68*, 104272.
- [9] S. L. Zhang, Y.-C. Lai, X. He, R. Liu, Y. Zi, Z. L. Wang, *Adv. Funct. Mater.* **2017**, *27*, 1606695.
- [10] K. Dong, J. Deng, Y. Zi, Y.-C. Wang, C. Xu, H. Zou, W. Ding, Y. Dai, B. Gu, B. Sun, Z. L. Wang, *Adv. Mater.* **2017**, *29*, 1702648.
- [11] J. Chen, J. Yang, Z. Li, X. Fan, Y. Zi, Q. Jing, H. Guo, Z. Wen, K. C. Pradel, S. Niu, Z. L. Wang, *ACS Nano* **2015**, *9*, 3324.
- [12] Q. Liang, Q. Zhang, X. Yan, X. Liao, L. Han, F. Yi, M. Ma, Y. Zhang, *Adv. Mater.* **2017**, *29*, 1604961.
- [13] H.-J. Kim, E.-C. Yim, J.-H. Kim, S.-J. Kim, J.-Y. Park, I.-K. Oh, *Nano Energy* **2017**, *33*, 130.
- [14] C. Yao, A. Hernandez, Y. Yu, Z. Cai, X. Wang, *Nano Energy* **2016**, *30*, 103.
- [15] C. Yao, X. Yin, Y. Yu, Z. Cai, X. Wang, *Adv. Funct. Mater.* **2017**, *27*, 1700794.
- [16] K. Shi, X. Huang, B. Sun, Z. Wu, J. He, P. Jiang, *Nano Energy* **2019**, *57*, 450.
- [17] Q. Zheng, H. Zhang, H. Mi, Z. Cai, Z. Ma, S. Gong, *Nano Energy* **2016**, *26*, 504.
- [18] C. Qian, L. Li, M. Gao, H. Yang, Z. Cai, B. Chen, Z. Xiang, Z. Zhang, Y. Song, *Nano Energy* **2019**, *63*, 103885.
- [19] H. Zou, Y. Zhang, L. Guo, P. Wang, X. He, G. Dai, H. Zheng, C. Chen, A. C. Wang, C. Xu, Z. L. Wang, *Nat. Commun.* **2019**, *10*, 1427.
- [20] J. Luo, Z. Wang, L. Xu, A. C. Wang, K. Han, T. Jiang, Q. Lai, Y. Bai, W. Tang, F. R. Fan, Z. L. Wang, *Nat. Commun.* **2019**, *10*, 5147.
- [21] H. Oh, S. S. Kwak, B. Kim, E. Han, G. Lim, S. Kim, B. Lim, *Adv. Funct. Mater.* **2019**, *29*, 1904066.
- [22] B. N. Chandrashekar, B. Deng, A. S. Smitha, Y. Chen, C. Tan, H. Zhang, H. Peng, Z. Liu, *Adv. Mater.* **2015**, *27*, 5210.
- [23] S. Kim, M. K. Gupta, K. Y. Lee, A. Sohn, T. Y. Kim, K.-S. Shin, D. Kim, S. K. Kim, K. H. Lee, H.-J. Shin, D.-W. Kim, S.-W. Kim, *Adv. Mater.* **2014**, *26*, 3918.
- [24] Y. Zi, H. Guo, J. Wang, Z. Wen, S. Li, C. Hu, Z. L. Wang, *Nano Energy* **2017**, *31*, 302.
- [25] L. Dhakar, P. Pitchappa, F. E. H. Tay, C. Lee, *Nano Energy* **2016**, *19*, 532.

- [26] Z. Wen, M.-H. Yeh, H. Guo, J. Wang, Y. Zi, W. Xu, J. Deng, L. Zhu, X. Wang, C. Hu, L. Zhu, X. Sun, Z. L. Wang, *Sci. Adv.* **2016**, *2*, e1600097.
- [27] J. Chen, X. Pu, H. Guo, Q. Tang, L. Feng, X. Wang, C. Hu, *Nano Energy* **2018**, *43*, 253.
- [28] X. Wang, Y. Yang, *Nano Energy* **2017**, *32*, 36.
- [29] Y. Zi, H. Guo, Z. Wen, M.-H. Yeh, C. Hu, Z. L. Wang, *ACS Nano* **2016**, *10*, 4797.
- [30] Y. Xie, S. Wang, S. Niu, L. Lin, Q. Jing, J. Yang, Z. Wu, Z. L. Wang, *Adv. Mater.* **2014**, *26*, 6599.
- [31] G. Zhu, J. Chen, Y. Liu, P. Bai, Y. S. Zhou, Q. Jing, C. Pan, Z. L. Wang, *Nano Lett.* **2013**, *13*, 2282.
- [32] Y. Bian, T. Jiang, T. Xiao, W. Gong, X. Cao, Z. Wang, Z. L. Wang, *Adv. Mater. Technol.* **2018**, *3*, 1700317.
- [33] S. Park, H. Kim, M. Vosgueritchian, S. Cheon, H. Kim, J. H. Koo, T. R. Kim, S. Lee, G. Schwartz, H. Chang, Z. Bao, *Adv. Mater.* **2014**, *26*, 7324.
- [34] G. Zhu, Y. S. Zhou, P. Bai, X. S. Meng, Q. Jing, J. Chen, Z. L. Wang, *Adv. Mater.* **2014**, *26*, 3788.
- [35] J. Chun, B. U. Ye, J. W. Lee, D. Choi, C.-Y. Kang, S.-W. Kim, Z. L. Wang, J. M. Baik, *Nat. Commun.* **2016**, *7*, 12985.
- [36] J. Yang, C. Dahlström, H. Edlund, B. Lindman, M. Norgren, *Cellulose* **2019**, *26*, 3763.
- [37] J. Yang, J. Duan, L. Zhang, B. Lindman, H. Edlund, M. Norgren, *Cellulose* **2016**, *23*, 3105.
- [38] M. From, P. T. Larsson, B. Andreasson, B. Medronho, I. Svanedal, H. Edlund, M. Norgren, *Carbohydr. Polym.* **2020**, *236*, 116068.
- [39] M. F. Ashby, Y. J. M. Bréchet, *Acta Mater.* **2003**, *51*, 5801.
- [40] E. Rojo, M. S. Peresin, W. W. Sampson, I. C. Hoeger, J. Vartiainen, J. Laine, O. J. Rojas, *Green Chem.* **2015**, *17*, 1853.
- [41] I. González, M. Alcalà, G. Chinga-Carrasco, F. Vilaseca, S. Boufi, P. Mutjé, *Cellulose* **2014**, *21*, 2599.
- [42] L. Wågberg, G. Decher, M. Norgren, T. Lindström, M. Ankerfors, K. Axnäs, *Langmuir* **2008**, *24*, 784.
- [43] C. Dahlström, V. López Durán, S. T. Keene, A. Salleo, M. Norgren, L. Wågberg, *Carbohydr. Polym.* **2020**, *233*, 115829.
- [44] J. Patiño-Masó, F. Serra-Parareda, Q. Tarrés, P. Mutjé, F. X. Espinach, M. Delgado-Aguilar, *Nanomaterials* **2019**, *9*, 1271.
- [45] S. Chen, J. Jiang, F. Xu, S. Gong, *Nano Energy* **2019**, *61*, 69.
- [46] G. Y. Yun, H. S. Kim, J. Kim, K. Kim, C. Yang, *Sens. Actuators, A* **2008**, *141*, 530.
- [47] S. Yun, J. H. Kim, Y. Li, J. Kim, *J. Appl. Phys.* **2008**, *103*, 083301.
- [48] L. Csoka, I. C. Hoeger, O. J. Rojas, I. Peszlen, J. J. Pawlak, P. N. Peralta, *ACS Macro Lett.* **2012**, *1*, 867.